

 Open access • Posted Content • DOI:10.1101/620716

Insect herbivory reshapes a native leaf microbiome — [Source link](#)

[Parris T. Humphrey](#), [Parris T. Humphrey](#), [Parris T. Humphrey](#), [Noah K. Whiteman](#) ...+2 more authors

Institutions: [Harvard University](#), [University of Arizona](#), [Rocky Mountain Biological Laboratory](#), [University of California, Berkeley](#)

Published on: 26 Apr 2019 - [bioRxiv](#) (Cold Spring Harbor Laboratory)

Topics: [Population](#), [Microbiome](#) and [Phyllosphere](#)

Related papers:

- [Insect herbivory reshapes a native leaf microbiome.](#)
- [Herbivory shapes the rhizosphere bacterial microbiota in potato plants.](#)
- [Genetics-based interactions among plants, pathogens, and herbivores define arthropod community structure](#)
- [Tree diversity and functional leaf traits drive herbivore-associated microbiomes in subtropical China](#)
- [The Effect of Host-Plant Phylogenetic Isolation on Species Richness, Composition and Specialization of Insect Herbivores: A Comparison between Native and Exotic Hosts](#)

Share this paper:    

View more about this paper here: <https://typeset.io/papers/insect-herbivory-reshapes-a-native-leaf-microbiome-233j5273y5>

Insect herbivory reshapes a native leaf microbiome

Parris T Humphrey^{1,3,4,*} and Noah K Whiteman^{2,3,4}

¹Organismic & Evolutionary Biology, Harvard University, Cambridge, MA 02138 USA.

²Integrative Biology, University of California, Berkeley, CA 91604 USA.

³Rocky Mountain Biological Laboratory, Crested Butte, CO 81224 USA.

⁴Ecology & Evolutionary Biology, University of Arizona, Tucson, AZ 85721 USA.

2019-September-25

Abstract

Insect herbivory is pervasive in plant communities, but its impact on microbial plant colonizers is not well-studied in natural systems. By calibrating sequencing-based bacterial detection to absolute bacterial load, we find that the within-host abundance of most leaf microbiome (phyllosphere) taxa colonizing a native forb is amplified within leaves impacted by insect herbivory. Herbivore-associated bacterial amplification reflects community-wide compositional shifts towards lower ecological diversity, but the extent and direction of such compositional shifts can be interpreted only by quantifying absolute abundance. Experimentally eliciting anti-herbivore defenses reshaped within-host fitness ranks among *Pseudomonas* spp. field isolates and amplified a subset of putative *P. syringae* phytopathogens in a manner causally consistent with observed field-scale patterns. Herbivore damage was inversely correlated with plant reproductive success and was highly clustered across plants, which predicts tight co-clustering with putative phytopathogens across hosts. Insect herbivory may thus drive the epidemiology of plant-infecting bacteria as well as the structure of a native plant microbiome by generating variation in within-host bacterial fitness at multiple phylogenetic and spatial scales. This study emphasizes that “non-focal” biotic interactions between hosts and other organisms in their ecological settings can be crucial drivers of the population and community dynamics of host-associated microbiomes.

Keywords: co-infection, *Pseudomonas*, Brassicaceae, phyllosphere, microbiome, indirect interactions

Author Contributions: PTH and NKW designed the study. PTH carried out the study and analyzed the data. PTH and NKW wrote the manuscript. The authors declare that they have no conflicts of interest.

Data Availability: See <https://github.com/phumph/coinfection> for all scripts and raw input data. Saved model objects can be found archived in a Dryad repository (DOI pending). Sequence data can be found at the NIH Sequence Read Archive under project ID (pending).

Article type: Research Article

Running title: Herbivory and the phyllosphere

*Author for correspondence: PTH
e-mail: phumphrey@fas.harvard.edu

1 Introduction

2 For many organisms, attack by multiple enemies is inevitable and often occurs sequentially during the
3 lifetime of individual hosts. Prior attack can alter host phenotypes and change how future attacks unfold,
4 often generating cascading effects at larger spatial and temporal scales¹⁻⁴. Given the large effects of
5 co-infection on host health and the population dynamics of their parasites, explicitly studying co-infection
6 is becoming increasingly common⁴⁻⁶. But rarely has this perspective been extended to studies of diverse
7 host-associated microbial communities ('microbiomes'). Instead, microbiome studies tend to focus on
8 effects of host genotype or abiotic variation on microbiome diversity patterns⁷⁻¹¹. This has left a major
9 gap in our understanding of how host colonization from non-microbial enemies impacts the population
10 biology of microbiome-associated taxa.

11 For plants, there is tremendous interest in understanding the structure and function of the
12 microbiome both for applied purposes, such as engineering growth promotion and disease resistance^{12,13},
13 and as model systems for host-microbial symbioses more generally. Insect herbivory represents a pervasive
14 threat to plants in both native and agricultural settings¹⁴. Herbivory alters plant phenotypes through
15 tissue damage and induction of plant defenses, which can change susceptibility of plants to attack by
16 insects¹⁵ as well as microbes^{16,17}. Thus, factors that influence the impact of herbivores on hosts will likely
17 affect the colonization and growth of plant-associated microbes. While insect herbivores¹⁴ and
18 plant-associated microbes have clear effects on plant phenotypes and fitness¹⁸, they are generally
19 considered independently. Our study addresses this gap by explicitly considering how patterns of
20 abundance and diversity of leaf-colonizing (endophytic) bacterial taxa are altered in the presence of insect
21 herbivory and by exploring the associations among herbivory, bacterial infection, and plant fitness in a
22 native forb (*Cardamine cordifolia*, Brassicaceae; 'bittercress').

23 We first used marker gene sequencing (16S rRNA) coupled with paired leaf culturing to establish and
24 validate sequence-based estimates of absolute bacterial load in host tissue. By elucidating a relationship
25 between bacterial load and the sequence counts of bacteria- versus host-derived 16S (**Box 1**), our approach
26 enabled standard 16S marker gene sequencing to quantitatively reveal variation in abundance distributions
27 of entire suites of bacterial taxa across hosts with and without prior insect herbivory. We then assessed the
28 extent of co-clustering between microbial abundance and intensity of insect herbivory at the plant patch
29 scale across our study populations, and we related microbe-herbivore co-aggregation to fruit set, a
30 component of plant fitness. In parallel, we directly examined variation in sensitivity to inducible plant
31 defenses among 12 genetically diverse, bittercress-derived isolates of *Pseudomonas* spp. bacteria. We did so

32 by experimentally infecting accessions of native bittercress in the laboratory in which prior herbivory was
33 simulated by exogenously pre-treating plants with the plant defense hormone jasmonic acid (JA).

34 Our experiments reveal that insect herbivory, via induction of plant defenses, can modify endophytic
35 bacterial diversity patterns by amplifying naturally prevalent and potentially phytopathogenic bacterial
36 taxa within a native plant host. This mechanism may be at least partly responsible for the strong positive
37 association between herbivory and endophytic bacterial abundance within leaf microbiomes seen under field
38 conditions. Crucially, the patterns and degree of bacterial abundance variation we found cannot be
39 revealed by traditional compositional analysis of high-throughput marker gene sequencing, which masks
40 the extent and direction of within-host variation in bacterial load. By linking marker gene counts to an
41 absolute standard, our study reveals how insect herbivory associates with variation in bacterial loads at
42 leaf and patch scales within a natural plant population. More generally, this work highlights the
43 importance of (a) accounting for prevalent but "non-focal" biotic interactions hosts have with other
44 colonizers in their natural contexts, and (b) using detection and analytical approaches to quantify these
45 effects on components of microbial fitness.

46 **Methods**

47 **Field studies of herbivore–bacteria co-infection**

48 We surveyed herbivore damage arising from the specialist leaf-mining insect *Scaptomyza nigrita*
49 (Drosophilidae; Fig. S1f–g) in replicate 0.5 m² plots of native bittercress along transects in sub-alpine and
50 alpine streams near the Rocky Mountain Biological Laboratory (RMBL) in each of two years (2012,
51 Emerald Lake, EL, $n = 24$ plots; 2013, site North Pole Basin, NP, $n = 60$ plots; Fig. S1a–d). Although not
52 our primary focus, these field studies were also designed to test how mid-season pre-treatment with the
53 exogenous plant defense hormones JA or salicylic acid (SA) impacts plant attack rates by *S. nigrita*. JA
54 induces canonical defenses against chewing herbivores in plants¹⁷, including bittercress, and JA-induced
55 bittercress can locally deter adult *S. nigrita* and reduce larval feeding rates¹⁹. SA treatment canonically
56 induces defenses against biotrophic microbial colonizers and often pleiotropically suppresses plant defenses
57 against chewing herbivores¹⁷, including *S. nigrita*²⁰. Thus, treatment with either plant defense hormone
58 has the potential to modify the foraging behavior of *S. nigrita*. Our analysis of the impact of hormone
59 treatments on *S. nigrita* foraging patterns was previously published for site EL²⁰, and we implemented a
60 similar approach for site NP in this study. Full experimental design details are given in the Supplemental

61 Methods and are depicted in the schematic in Fig. S1e.

62 By the end of the growing season, when herbivory and bacterial infection had run their course, we
63 determined *S. nigrita* leaf-miner damage status of all leaves (both sites) as well as fruit set (site NP only)
64 produced on each of the focal bittercress stems (stem-level sample size $n = 768$, site EL; $n = 1920$, site
65 NP). At both sites, we collected leaf tissue in a randomized manner (see Supplemental Methods) to
66 quantify the abundance and diversity of bacteria that had colonized the leaf interior.

67 **Amplicon sequencing of bacteria in leaf tissues**

68 We quantified bacterial abundance in leaf tissues using next-generation amplicon sequencing of the
69 bacterial 16S rRNA locus using the Illumina MiSeq platform. In order to enrich our samples for endophytic
70 bacteria, we surface-sterilized all samples prior to DNA extraction, which achieved a reliable reduction of
71 bacterial abundance as detected by our 16S analysis approach (Fig. S2). Subsequently, we extracted DNA
72 from the 192 leaf discs ($\sim 0.8 \text{ cm}^2$) from site EL and 192 tissue pools from site NP (4 four discs per pool)
73 and amplified bacterial 16S following protocol established for the Earth Microbiome Project (see
74 Supplemental Methods). We amended this protocol by including peptic nucleic acid (PNA) PCR clamps
75 into reaction mixtures to reduce amplification of host chloroplast- and mitochondria-derived 16S, following
76 Lundberg et al.²¹. This was highly effective at reducing the proportion of host-derived 16S reads per
77 library in our sample sets (Fig. S3).

78 We then used DADA2²² to error-correct, trim, quality-filter, and merge the paired-end sequencing reads
79 that passed error thresholds off the sequencer. Of the approximately 4 million raw reads, $\sim 90\%$ were
80 retained following quality control via DADA2 (Fig. S4), and these reads were then delineated into exact
81 amplicon sequencing variants (ASVs). 16S reads from bittercress chloroplast or mitochondria were
82 manually curated and summed into ‘host-derived’ for comparison with bacteria-derived 16S (see
83 Supplemental Methods).

84 **Quantifying and modeling bacterial abundance patterns**

85 In order to quantitatively assess how herbivore damage relates to abundance and diversity of microbial
86 plant colonizers, we required a link between 16S counts and bacterial load. We therefore devised and
87 validated an estimator (γ) of the abundance of bacterial ASVs within host tissues (**Box 1**). Using γ as an
88 empirically validated estimator of absolute bacterial load in leaf tissues, we then constructed a two-stage
89 modeling approach to estimate bacterial load across our complete sample set.

90 We first fit and compared a series of increasingly flexible Bayesian regression models to estimate how
91 γ varies as a function of herbivore damage in leaves (see Supplemental Methods). When calculating γ , we
92 took r_B at the bASV-level for all bASVs within each of the 14 most abundant bacterial families, together
93 comprising $> 95\%$ of total bASV counts in the datasets. We then took the candidate best stage-1 model,
94 heuristically defined as the model with the lowest leave-one-out Bayesian information criterion
95 (LOO-IC)²³, and used it to generate $n = 200$ replicate sets of simulated response values ($\tilde{\gamma}$) predicted by
96 the model parameters fit to the original data.

97 In the next stage, we used this distribution of $\tilde{\gamma}$ as an input predictor variable to the model we fit
98 between our observed γ and observed log CFU (**Box 1**). This allowed us to report bacterial abundance
99 estimates, based initially on 16S count data, on the scale of predicted log CFU per unit leaf mass—a more
100 directly interpretable measure of within-host fitness. Rather than point estimates, we sampled intercept,
101 slope, and residual error parameters from their joint posterior distribution of the calibration CFU model
102 for each data point independently. Specifically, this has the effect of incorporating noise in the fit between
103 observed log CFU and γ such that downstream predictions are not overly biased by the precise value of any
104 regression slope estimate, which may itself arise from peculiarities in the action of PNA during
105 amplification of 16S. Overall, this two-stage modeling approach was designed to incorporate uncertainty in
106 the model fit for γ as well as in the relationship between observed γ and observed log CFU. The endpoint
107 of this approach is 200 sets of posterior predicted log CFU values for each sample in the dataset, which
108 formed the basis of downstream calculations of bacterial abundance variation, as well as ecological diversity
109 (Shanon evenness J') and similarity (Shannon–Jensen divergence SJ) in and between damaged and
110 undamaged leaf sets, respectively (see Supplemental Methods).

111 **Population-level analysis of herbivore–bacteria co-aggregation**

112 We assessed how patch-level variation in herbivory correlated with bacterial infection intensity at the
113 field-scale by focusing on the most highly abundant bASV at both field sites ('Pseudomonas3'). Leaf-level
114 abundance of this individual bASV was predicted using the approach described above. We then summed
115 the predicted abundance (on the linear scale) of bacteria across leaves within each plant patch and used
116 these predicted bacterial sums to calculate the cumulative proportion of the total Pseudomonas3
117 population harbored by plant patches with differing levels of herbivory, which portrays the extent of
118 co-aggregation of herbivores and bacteria across the host population.

119 **Experimental infections *in planta***

120 We directly examined how inducible plant defenses against chewing herbivores impacted within-host
121 bacterial performance using field-derived accessions of bittercress plants and their bacterial colonizers. We
122 randomized the selection of six focal strains from within each of the two dominant *Pseudomonas* clades (*P.*
123 *syringae*, and *P. fluorescens*) represented in our endophytic strain collection from bittercress²⁰. We
124 infected each strain into a single leaf on each of $n = 32$ distinct bittercress clones that had been
125 randomized to receive pre-treated 3 days prior with JA (1 mM; Sigma) or a mock solution. Bittercress
126 clones were originally isolated as rhizomes from various sites within 2 km of the RMBL in 2012 and were
127 re-grown in the greenhouse at University of Arizona for up to 12 months prior to use²⁴. Two days post
128 infection, we sampled, sterilized, homogenized, and dilution-plated leaf discs onto non-selective rich King's
129 B media, following Humphrey et al.²⁰. We compared bacterial abundance (\log_2) between treated and
130 untreated samples using Gaussian Bayesian regression models. We subsequently used posterior predicted
131 abundances as the basis for considering how herbivore-inducible defenses impact the composition and
132 diversity of this *Pseudomonas* community at different taxonomic levels (see Supplemental Methods).

133 **Results**

134 **Bacterial loads are amplified in insect-damaged leaf tissues**

135 By linking information from 16S counts to absolute bacterial abundance (**Box 1**), we found that bacteria
136 detected within herbivore-damaged leaves exhibit local population sizes several doublings greater compared
137 to the bacteria found in undamaged leaves (Fig. 1a,b; median \pm 95% credible interval of posterior
138 predicted additional doublings: 2.5 [2.1; 3.9] site EL; 4.5 [3.6; 5.3] site NP). This result, rooted in sequence
139 data, is further validated by the parallel observation that damaged leaves showed higher bacterial loads
140 than undamaged leaves via culturing of the $n = 101$ calibration set (Fig. S5; mean difference of 3.7
141 bacterial doublings [1.8–5.6, 95% c.i. on mean difference]; Welch's unequal variance two-sample t -test,
142 $t = 3.86$, $p < 0.001$), which is quantitatively consistent with a prior result from a parallel and independent
143 culture-based study in this system²⁰.

144 **Herbivore-associated bacterial amplification is both community-wide and** 145 **taxon-specific**

146 We then capitalized on the high taxonomic resolution and sampling depth afforded by amplicon sequencing
147 to examine shifts in abundance and distribution of diverse bacteria within the bittercress leaf microbiome.
148 Within-host density of bacterial bASVs from several bacterial families was elevated in herbivore-damaged
149 leaves compared to undamaged leaves (Fig. 1). For most families, the relative increase in within-host
150 density with herbivory was greater at site NP than at site EL (Fig. 1b), but this was largely because
151 several taxa showed lower baseline loads in undamaged leaves at site NP compared to site EL (Fig. S6a).
152 In contrast, bacterial loads for all families were similar for damaged leaves at both site (Fig. S6a,b).
153 Pseudomonadaceae was the most abundant taxon across all leaves and also showed the greatest fold
154 increase under herbivory (Fig. 1).

155 Several family-level γ models showed support for bASV-level differences in intercept and slope values
156 (Table S2), including Pseudomonadaceae and Sphingomonadaceae. Two individual bASVs in particular
157 drove family-level patterns in these clades (Fig. S7), which together comprised $\sim 20\%$ of all sequencing
158 reads across the two sample sets. Within the Pseudomonadaceae, *Pseudomonas3* was the most abundant
159 bASV, which falls within the putatively phytopathogenic *P. syringae* clade (Fig. S8). We previously
160 showed that *P. syringae* strains can be pathogenic, induce chlorosis, and reduce leaf photosynthetic
161 function in bittercress²⁰. Thus, a major component of the signal of elevated bacterial load in the presence
162 of insect herbivory comes from putatively phytopathogenic genotypes within the group *P. syringae*.

163 **Compositional shifts in leaf bacterial communities under herbivory**

164 When the absolute bacterial abundance patterns described above were analyzed in a compositional
165 framework, we detected differences in overall community structure and ecological diversity between
166 damaged and undamaged leaves. Specifically, we found lower evenness (J' ; Fig. 2b) in damaged leaves,
167 indicating a stronger skew towards a smaller number of bacterial taxa: Pseudomonadaceae comprise an
168 even greater proportion of the population in damaged leaves owing to their already-high average abundance
169 in undamaged leaves and large fold-increase under herbivory. Family-level relative abundances differed in
170 terms of Shannon–Jensen divergence (i.e., β -diversity) between damaged versus un-damaged leaves (Fig.
171 2c), indicating that amplification of bacteria in herbivore-damaged leaves can produce community-wide
172 signatures of reduced within-host diversity and elevated between-host diversity at broad taxonomic scales.

173 **Plant defenses against chewing herbivores enhance growth of putative**
174 **phytopathogens *in planta***

175 Plant pre-treatment with the plant defense hormone JA caused statistically clear alterations in within-host
176 growth of five of the twelve *Pseudomonas* spp. strains tested (Fig. 3a), with the most pronounced changes
177 resulting in 2.5–5 additional doublings of two phylogenetically distinct *P. syringae* isolates (20A and 02A;
178 Table S3). Increased within-host density of these two strains can account for differences in total
179 *Pseudomonas* abundance, as well as differences in abundance patterns summed at the level of bacterial
180 clade (*P. syringae* versus *P. fluorescens*; Fig. 3b). By recapitulating the elevated *P. syringae* and
181 family-wide increased abundance under herbivory seen in our field studies, this greenhouse result highlights
182 that induction of plant defenses against chewing herbivores is one potential mechanism whereby insect
183 herbivory could lead to amplification of bacterial taxa within the bittercress leaf microbiome.

184 Notably, two strains (22B and 20B) exhibited markedly decreased within-host fitness in JA-treated
185 compared to mock-treated leaves (Fig. 3a–b). Such herbivore-driven fitness variation among *P. syringae* is
186 undetectable when only considering larger taxonomic scales of genus or family (Fig. 3), where genotypes
187 which *increase* in local abundance contribute to an overall signature of elevated taxon-wide abundance as
188 measured by lower resolution tools (e.g., 16S sequencing). Thus, induction of plant defenses against
189 chewing herbivores leads to the amplification and numerical dominance of a narrow subset of the *P.*
190 *syringae* community within this host population (Fig. 3c). Such changes result in compositional shifts
191 towards decreased Shannon evenness in JA-treated leaves (Fig. 3d) and an overall community-wide
192 divergence with mock-treated leaves (Fig. 3e).

193 **Putative phytopathogens are aggregated in highly herbivore-damaged plant**
194 **patches**

195 We then analyzed how *Pseudomonas3*, a highly abundant individual bASV within the *P. syringae* group,
196 varied across bittercress plant patches in relation to the level of herbivory on those plant patches. At site
197 NP, we found a highly aggregated (i.e., right-skewed) distribution of herbivore loads across plant patches
198 (Fig. 4a, top marginal density plot). This aggregated herbivore distribution across plant patches results in
199 a predicted 50-fold enrichment of local density of *Pseudomonas3* in the most-damaged compared to the
200 least-damaged plant patch (Fig. 4). Analyzed in a more general framework, over half the predicted
201 *Pseudomonas3* population is harbored in just one fifth of the plant patches in the bittercress population at

202 our study site NP (Fig. S9).

203 **Herbivore–bacteria co-aggregation is associated with lower plant fitness**

204 At site NP, bittercress patches with higher herbivore intensity showed lower reproductive success, with the
205 most damaged patches estimated to produce half as many fruits as patches with no herbivore damage (Fig.
206 4b, Table S4). Plants with more insect damage tend to have higher levels of bacterial infection. Thus,
207 standing variation in fruit set is closely associated with levels of co-aggregation of these plant natural
208 enemies across our sample within this native bittercress population.

209 **Causes of herbivore aggregation in natural plant populations**

210 The degree of herbivore aggregation among host plants at site NP varied extensively across plant patches
211 at site NP (Fig. S10a–b); the marginal effects on herbivore damage arising from early-season treatments
212 with plant defense hormones SA or JA were small (Fig. S10c). Estimates for both SA and JA treatment
213 coefficients were elevated above the mock/control condition, but the posterior distribution for both
214 hormone effects overlapped zero (lower 4th %-ile < 0 for JA; lower 15th %-ile < 0 for SA; Table S5). Thus,
215 while prior plant exposure to JA, and possible also SA, may cause elevated *S. nigrita* herbivory at the
216 patch scale, standing variation in *S. nigrita* herbivory arising stochastically or from unmeasured factors at
217 site NP dominates over any causal effects of our population-level defense hormone manipulation.
218 Additionally, these plant-level defense hormone treatments (five weeks prior to leaf sampling) showed no
219 discernible effect on distributions of γ for overall or family-wise bacterial abundance (Fig. S11).

220 **Discussion**

221 **Overview**

222 Here we show that insect herbivory is strongly associated with bacterial abundance and diversity within a
223 native plant microbiome using field and greenhouse experiments. We provide evidence that activation of
224 plant defenses against chewing herbivores is at least one causal mechanism whereby such within-host
225 amplification of leaf-colonizing bacteria can occur. Specifically, the growth of a majority of bacterial taxa
226 found in the leaf microbiome of native bittercress was amplified in plant tissues damaged by the specialist
227 herbivore *S. nigrita* (Fig. 1) at two separate sub-alpine field sites. These ecological effects were only

228 detectable by linking sequence-based bacterial quantification to an external standard of absolute
229 abundance (**Box 1**), rather than relying on compositional analysis as is commonly done with studies of
230 both plant and animal microbiomes (but see Vandeputte et al.²⁵).

231 The bacterial clades most altered under herbivory include strains from groups well-known for causing
232 plant disease (*P. syringae*), and our follow-up experimental work in the greenhouse showed that inducing
233 plant defenses against chewing herbivores in bittercress was sufficient to cause similar degrees of
234 amplification of putatively phytopathogenic *P. syringae* genotypes in leaf tissues. Amplification of specific
235 *P. syringae* genotypes can largely account for species- and family-level patterns seen in our field studies,
236 which has coarser taxonomic resolution. Overall, these experiments suggest that *S. nigrita* herbivores may
237 play a larger role than previously appreciated in promoting the within-host growth of particular bacterial
238 genotypes or pathovars in bittercress, although the causal nature of the role of herbivores was not gleaned
239 from the field portion of this study. Given that the majority of plants face herbivore attack to some
240 degree^{14,26}, it is possible that our results generalize across plant-microbe systems.

241 **Herbivore-inducible plant defenses can amplify putative phytopathogens**

242 The mechanisms governing growth-promoting effects of insect herbivory on leaf-colonizing bacteria are
243 potentially numerous. Leaf damage itself can release nutrients, alleviating resource constraints for bacteria
244 while also creating routes for colonization of the leaf interior from the leaf surface^{27,28}. Plant defenses
245 induced by chewing herbivores could directly or indirectly alter interactions with bacteria independent of
246 the physical effects of plant tissue damage. It is known that JA-dependent anti-herbivore defenses can
247 suppress the subsequent activity of signaling pathways responsive to bacterial infection¹⁷, allowing bacteria
248 (including strains of *P. syringae*) to reach higher densities within JA-affected leaf tissues²⁹. Insects such as
249 *S. nigrita* trigger such JA-dependent host defenses in bittercress¹⁹, and this form of defense signaling is
250 widely conserved among diverse plant groups¹⁷. Released from top-down control, a diversity of resident
251 microbes can then proliferate as defenses are more strongly directed against herbivory, which may manifest
252 in community-wide patterns of abundance changes as noted in our study (Fig. 1).

253 The hypothesis that anti-herbivore defenses pleiotropically increase bacterial growth is consistent with
254 results from our greenhouse experiment. We found that the within-host fitness of several strains of
255 putatively phytopathogenic *P. syringae* increased within bittercress leaves pre-treated with JA compared
256 to mock-treated leaves (Fig. 2). Although our experiment is consistent with this plausible mechanism by
257 which herbivores can facilitate bacterial growth within plants, it does not identify the proximal

258 mechanism(s) responsible for these effects. JA-induced defenses may have instead stressed the plants,
259 decreasing basal tolerance to infection, or shunted resources towards investments which reduce the ability
260 of plants to resist or tolerate bacterial infection³⁰. Such net effects of JA induction on bacterial abundance
261 are likely contingent on underlying constitutive levels of genetic resistance and/or tolerance to herbivory,
262 traits which often exhibit quantitative variation within and among plant populations³¹. The role of host
263 genetic variation in defense responsiveness phenotypes in mediating the impacts of herbivore attack on
264 microbial plant colonization is an open avenue of future research.

265 Finally, several other abundant bacterial groups (e.g., Sphingomonadaceae, Flavobacteriaceae)
266 exhibited amplified abundance under insect herbivory in our field studies (Fig. 1). Functional studies
267 examining finer-scale variation among genotypes of these relatively less well-studied bacterial groups would
268 be highly fruitful for establishing a more general understanding of the mechanistic basis of plant–microbe
269 interactions in the context of inducible defenses against chewing herbivores.

270 **Herbivore distributions can alter the spatial patterning of plant disease**

271 The impact of insect herbivory on phyllosphere bacteria can be observed at several spatial scales.
272 Herbivore damage was highly clustered on a subset of hosts (Fig. 4), which is a pattern consistent with
273 other plant–herbivore systems³² as well as many host–macroparasite systems more generally³³. A potential
274 accompanying effect of aggregated herbivore damage is to enrich bacterial infection on a subset of the host
275 population (Fig. 4, Fig. S8), altering the spatial structure of growth and, potentially, transmission of
276 plant-colonizing microbes. Uncovering the temporal dynamics of how herbivore aggregation precedes or
277 follows microbial attack—or whether the two colonizers cyclically amplify one another—will require more
278 controlled studies that manipulate the timing and density of herbivory itself.

279 Regardless of the precise mechanisms resulting in such herbivore–microbe co-aggregation, plant
280 patches with the highest levels of co-aggregation had substantially (~ 50%) lower reproductive success
281 compared to minimally-damaged plant patches (Fig. 4b). Although we cannot identify the cause of lower
282 plant fitness from our study, the co-aggregation of these distinct plant colonizers may at least partly
283 explain it. Whether these plants were more stressed to begin with or achieved lower fruiting success
284 because of their infestation with herbivores and phytopathogens cannot be resolved without future studies
285 which isolate the causal effects of single and multiple infection on plant fitness.

286 What drives the highly skewed pattern of herbivory among host plants? Plant populations often
287 display a patchwork of defensive phenotypes, influenced by plant abiotic stress, variation in the underlying

288 defensive alleles, or by defense induction from prior herbivore or microbial attack. While plant defenses can
289 shape herbivore attack rates in the laboratory and over wide spatial extents³¹, less is known about how
290 patterns of defense induction impact the population dynamics of insect herbivores^{32,34}. Many insects are
291 deterred by anti-herbivore defenses, but some specialist herbivores use these same cues as attractants owing
292 to detoxification mechanisms which confer resistance to such defenses³⁵. *S. nigrita* uses anti-herbivore
293 plant defenses to locate host but also avoids high concentrations of defensive compounds when given the
294 option¹⁹. Thus, the joint expression of positive chemo-taxis towards JA-inducible compounds, coupled to
295 aversion of high levels of JA responsive defensive chemistry, may influence where herbivory becomes
296 concentrated among plants in native bittercress populations.

297 Results from our field hormone treatments using JA and SA both showed elevated patch-level *S.*
298 *nigrita* leaf miner damage compared to mock-treated patches (Fig. S10). However, the statistical signature
299 of these treatment effects was not clear enough to confidently conclude that our field trials substantially
300 altered natural patterns of herbivory by this specialist, given the high degree of stochastic or unexplained
301 variation in herbivore damage we observed across plant patches (Fig. S10, Table S5). Discovering the
302 biotic and abiotic factors structuring herbivory patterns in natural host populations thus remains a
303 challenge in this system³⁶ as well as many others³⁴, and we have not attempted to solve this problem in
304 the present study. Nonetheless, our study suggests that predicting herbivore distributions may be key for
305 understanding population-level distributions of plant-associated bacteria. Regardless of its causes, insect
306 herbivore damage can be readily measured and incorporated into plant microbiome studies in order to help
307 reveal the drivers of variation in microbiome abundance and diversity within plant communities.

308 **Quantifying bacterial loads is crucial for understanding the ecology of the** 309 **microbiome**

310 The patterns of abundance variation among bacterial taxa across leaf types, when distilled into a
311 community-level compositional metric, showed decreased ecological diversity (i.e., evenness) in damaged
312 versus un-damaged leaves, resulting in overall compositional divergence between sample sets (Fig. 2–3).
313 This results from particular taxa undergoing larger absolute changes in abundance than other taxa, which
314 leads to stronger skews in the composition of the community calculated on the relative scale.
315 Compositional analysis on its own would preclude inference of the direction or magnitude of changes in
316 bacterial abundance³⁷, even though this is of primary interest to researchers exploring the microbiome and
317 its impact on host fitness^{25,38,39}. Compositional methods are thus poorly suited to studies of the

318 population biology of microbiome-dwelling bacterial taxa when bacterial load varies or when microbial
319 fitness is a desired response variable.

320 Direct bacterial quantification²⁵, as well as controlled DNA spike-ins⁴⁰, can correct for biases and
321 ambiguities inherent to compositional analyses. Our study provides an additional and novel framework for
322 enabling standard high-throughput 16S sequencing approaches to provide quantitative measures of
323 bacterial abundance when canonical approaches (e.g., qPCR) are infeasible due to host organelle
324 contamination. Rather than being discarded, 16S read counts derived from host organelles—once
325 curated—can provide an internal reference population against which the proportionality of other taxa can
326 be measured⁴¹. While we have established the usefulness of our estimator of bacterial load (γ) using a
327 paired culture-based experiment, this need not be the only way. Bacterial culturing is an intrinsically noisy
328 means of enumerating bacteria, due to dilution and/or counting noise. In addition, chemically-mediated
329 antagonism or facilitation among bacterial species can cause over- or under-detection of particular
330 combinations of taxa on agar plates⁴². These limitations will no doubt set a lower limit to the resolution of
331 biological effects one is capable of detecting with culture-dependent methods. Testing the generality of our
332 approach across other plant–microbe systems, and with other means of enumerating bacteria in samples, is
333 therefore a priority.

334 Conclusions

335 Our study emphasizes that large effects on the population biology of *P. syringae*, and many other lineages
336 of leaf-colonizing bacteria, may stem from the action of insect herbivores. Biotic interactions such as
337 herbivory are absent from the classic ‘disease triangle’ of plant pathology. The role of insect herbivores in
338 *P. syringae* epidemiology—and plant–microbiome relations in general—has been under-appreciated.
339 Variation in bacterial abundance across samples, and the implications of relative abundance changes for
340 bacterial fitness, are not easily detectable via compositional analyses applied to 16S data, which typically
341 do not utilize external or internal standards. Thus, studies aiming to decipher why plant microbiomes
342 differ in structure or function should endeavor to quantify bacterial loads in order to retain this important
343 axis of variation as a focal response variable, while also considering additional biotic interactions commonly
344 encountered by the hosts under study.

345 Acknowledgements

346 PTH and NKW gratefully acknowledge funding from the National Science Foundation (DEB-1309493 to
347 PTH, DEB-1256758 to NKW), the National Institute of General Medical Sciences of the National
348 Institutes of Health (R35GM119816 to NKW), as well as the Rocky Mountain Biological Laboratory. We
349 are indebted to field assistance provided by Heather Briggs, Kara Cromwell, Aaron Koning, Lucy
350 Anderson, Kyle Niezgoda, Devon Picklum, and Nicolas Alexandre; bioinformatics advice from Tim K
351 O'Connor; and laboratory assistance from Hoon Pyon and Amir Abidov. We thank our contacts at
352 Argonne National Laboratory Sarah Owens and Jason Koval for their technical expertise and support.

353 References

- 354 [1] Lloyd-Smith J. O., Poss M., and Grenfell B. T. Hiv-1/parasite co-infection and the emergence of new
355 parasite strains. *Parasitology*, 135(7):795–806, Jun 2008. doi: 10.1017/S0031182008000292.
- 356 [2] Laine A.-L. Context-dependent effects of induced resistance under co-infection in a plant-pathogen
357 interaction. *Evol Appl*, 4(5):696–707, Sep 2011. doi: 10.1111/j.1752-4571.2011.00194.x.
- 358 [3] Tollenaere C., Susi H., and Laine A.-L. Evolutionary and epidemiological implications of multiple
359 infection in plants. *Trends Plant Sci*, 21(1):80–90, Jan 2016.
- 360 [4] Karvonen A., Jokela J., and Laine A.-L. Importance of sequence and timing in parasite coinfections.
361 *Trends Parasitol*, Dec 2018. doi: 10.1016/j.pt.2018.11.007.
- 362 [5] Halliday F. W., Umbanhowar J., and Mitchell C. E. Interactions among symbionts operate across
363 scales to influence parasite epidemics. *Ecol Lett*, 20:1285–1294, Sep 2017.
- 364 [6] Susi H., Barrès B., Vale P. F., and Laine A.-L. Co-infection alters population dynamics of infectious
365 disease. *Nat Commun*, 6:5975, Jan 2015. doi: 10.1038/ncomms6975.
- 366 [7] Horton M. W., Bodenhausen N., Beilsmith K., Meng D., Muegge B. D., Subramanian S., Vetter
367 M. M., Vilhjálmsson B. J., Nordborg M., Gordon J. I., and Bergelson J. Genome-wide association
368 study of arabidopsis thaliana leaf microbial community. *Nat Commun*, 5:5320, 2014.
- 369 [8] Bulgarelli D., Rott M., Schlaeppli K., Themaat E. Ver Loren van , Ahmadinejad N., Assenza F., Rauf
370 P., Huettel B., Reinhardt R., Schmelzer E., Peplies J., Gloeckner F. O., Amann R., Eickhorst T., and
371 Schulze-Lefert P. Revealing structure and assembly cues for arabidopsis root-inhabiting bacterial
372 microbiota. *Nature*, 488(7409):91–5, Aug 2012.
- 373 [9] Bodenhausen N., Bortfeld-Miller M., Ackermann M., and Vorholt J. A. A synthetic community
374 approach reveals plant genotypes affecting the phyllosphere microbiota. *PLoS Genet*, 10(4):e1004283,
375 Apr 2014.
- 376 [10] Edwards J., Johnson C., Santos-Medellín C., Lurie E., Podishetty N. K., Bhatnagar S., Eisen J. A.,
377 and Sundaresan V. Structure, variation, and assembly of the root-associated microbiomes of rice. *Proc*
378 *Natl Acad Sci U S A*, 112(8):E911–20, Feb 2015.

- 379 [11] Wagner M. R., Lundberg D. S., Del Rio T. G., Tringe S. G., Dangl J. L., and Mitchell-Olds T. Host
380 genotype and age shape the leaf and root microbiomes of a wild perennial plant. *Nat Commun*, 7:
381 12151, 2016.
- 382 [12] Finkel O. M., Castrillo G., Herrera Paredes S., Salas González I., and Dangl J. L. Understanding and
383 exploiting plant beneficial microbes. *Curr Opin Plant Biol*, 38:155–163, 08 2017. doi:
384 10.1016/j.pbi.2017.04.018.
- 385 [13] Orozco-Mosqueda M. D. C., Rocha-Granados M. D. C., Glick B. R., and Santoyo G. Microbiome
386 engineering to improve biocontrol and plant growth-promoting mechanisms. *Microbiol Res*, 208:25–31,
387 Mar 2018. doi: 10.1016/j.micres.2018.01.005.
- 388 [14] Maron J. L. and Crone E. Herbivory: effects on plant abundance, distribution and population growth.
389 *Proc Biol Sci*, 273(1601):2575–84, Oct 2006. doi: 10.1098/rspb.2006.3587.
- 390 [15] Agrawal A. A. Induced responses to herbivory and increased plant performance. *Science*, 279(5354):
391 1201–2, Feb 1998.
- 392 [16] Bressan M., Roncato M.-A., Bellvert F., Comte G., Haichar F. Z., Achouak W., and Berge O.
393 Exogenous glucosinolate produced by arabidopsis thaliana has an impact on microbes in the
394 rhizosphere and plant roots. *ISME J*, 3(11):1243–57, Nov 2009.
- 395 [17] Thaler J. S., Humphrey P. T., and Whiteman N. K. Evolution of jasmonate and salicylate signal
396 crosstalk. *Trends Plant Sci*, 17(5):260–70, May 2012. doi: 10.1016/j.tplants.2012.02.010.
- 397 [18] Wagner M. R., Lundberg D. S., Coleman-Derr D., Tringe S. G., Dangl J. L., and Mitchell-Olds T.
398 Natural soil microbes alter flowering phenology and the intensity of selection on flowering time in a
399 wild arabidopsis relative. *Ecol Lett*, 17(6):717–26, Jun 2014. doi: 10.1111/ele.12276.
- 400 [19] Humphrey P. T., Gloss A. D., Alexandre N. M., Villalobos M. M., Fremgen M. R., Groen S. C.,
401 Meihls L. N., Jander G., and Whiteman N. K. Aversion and attraction to harmful plant secondary
402 compounds jointly shape the foraging ecology of a specialist herbivore. *Ecol Evol*, 6(10):3256–68, 05
403 2016. doi: 10.1002/ece3.2082.
- 404 [20] Humphrey P. T., Nguyen T. T., Villalobos M. M., and Whiteman N. K. Diversity and abundance of
405 phyllosphere bacteria are linked to insect herbivory. *Mol Ecol*, 23(6):1497–515, Mar 2014. doi:
406 10.1111/mec.12657.
- 407 [21] Lundberg D. S., Yourstone S., Mieczkowski P., Jones C. D., and Dangl J. L. Practical innovations for
408 high-throughput amplicon sequencing. *Nat Methods*, 10(10):999–1002, Oct 2013. doi:
409 10.1038/nmeth.2634.
- 410 [22] Callahan B. J., McMurdie P. J., Rosen M. J., Han A. W., Johnson A. J. A., and Holmes S. P. Dada2:
411 High-resolution sample inference from illumina amplicon data. *Nat Methods*, 13(7):581–3, 07 2016.
412 doi: 10.1038/nmeth.3869.
- 413 [23] Vehtari A., Gelman A., and Gabry J. Practical bayesian model evaluation using leave-one-out
414 cross-validation and waic. *Statistics and Computing*, 27(5):1413–1432, Sep 2017. ISSN 1573-1375. doi:
415 10.1007/s11222-016-9696-4.
- 416 [24] Humphrey P. T., Gloss A. D., Frazier J., Nelson-Dittrich A. C., Faries S., and Whiteman N. K.
417 Heritable plant phenotypes track light and herbivory levels at fine spatial scales. *Oecologia*, 187(2):
418 427–445, Jun 2018. doi: 10.1007/s00442-018-4116-4.
- 419 [25] Vandeputte D., Kathagen G., D’hoë K., Vieira-Silva S., Valles-Colomer M., Sabino J., Wang J., Tito
420 R. Y., De Commer L., Darzi Y., Vermeire S., Falony G., and Raes J. Quantitative microbiome
421 profiling links gut community variation to microbial load. *Nature*, 551(7681):507–511, 11 2017. doi:
422 10.1038/nature24460.

- 423 [26] Turcotte M. M., Davies T. J., Thomsen C. J. M., and Johnson M. T. J. Macroecological and
424 macroevolutionary patterns of leaf herbivory across vascular plants. *Proc Biol Sci*, 281(1787), Jul
425 2014. doi: 10.1098/rspb.2014.0555.
- 426 [27] Hirano S. S. and Upper C. D. Bacteria in the leaf ecosystem with emphasis on pseudomonas
427 syringae—a pathogen, ice nucleus, and epiphyte. *Microbiol Mol Biol Rev*, 64(3):624–53, Sep 2000.
- 428 [28] Lindow S. E. and Brandl M. T. Microbiology of the phyllosphere. *Appl Environ Microbiol*, 69(4):
429 1875–83, Apr 2003.
- 430 [29] Cui J., Bahrami A. K., Pringle E. G., Hernandez-Guzman G., Bender C. L., Pierce N. E., and
431 Ausubel F. M. Pseudomonas syringae manipulates systemic plant defenses against pathogens and
432 herbivores. *Proc Natl Acad Sci U S A*, 102(5):1791–6, Feb 2005. doi: 10.1073/pnas.0409450102.
- 433 [30] Huang H., Liu B., Liu L., and Song S. Jasmonate action in plant growth and development. *J Exp Bot*,
434 68(6):1349–1359, 03 2017. doi: 10.1093/jxb/erw495.
- 435 [31] Züst T., Heichinger C., Grossniklaus U., Harrington R., Kliebenstein D. J., and Turnbull L. A.
436 Natural enemies drive geographic variation in plant defenses. *Science*, 338(6103):116–9, Oct 2012. doi:
437 10.1126/science.1226397.
- 438 [32] Underwood N., Anderson K., and Inouye B. D. Induced vs. constitutive resistance and the spatial
439 distribution of insect herbivores among plants. *Ecology*, 86(3):594–602, 2005.
- 440 [33] Shaw D. J. and Dobson A. P. Patterns of macroparasite abundance and aggregation in wildlife
441 populations: a quantitative review. *Parasitology*, 111 Suppl:S111–27, 1995.
- 442 [34] Karban R. and Baldwin I. T. *Induced Responses to Herbivory*. University of Chicago Press, 1997.
- 443 [35] Wittstock U., Agerbirk N., Stauber E. J., Olsen C. E., Hippler M., Mitchell-Olds T., Gershenzon J.,
444 and Vogel H. Successful herbivore attack due to metabolic diversion of a plant chemical defense. *Proc*
445 *Natl Acad Sci U S A*, 101(14):4859–64, Apr 2004. doi: 10.1073/pnas.0308007101.
- 446 [36] Alexandre N. M., Humphrey P. T., Gloss A. D., Lee J., Frazier J., Affeldt H. A., 3rd, and Whiteman
447 N. K. Habitat preference of an herbivore shapes the habitat distribution of its host plant. *Ecosphere*, 9
448 (9), Sep 2018. doi: 10.1002/ecs2.2372.
- 449 [37] Gloor G. B., Macklaim J. M., Pawlowsky-Glahn V., and Egozcue J. J. Microbiome datasets are
450 compositional: And this is not optional. *Frontiers in Microbiology*, 8:2224, 2017. doi:
451 10.3389/fmicb.2017.02224.
- 452 [38] Falony G., Joossens M., Vieira-Silva S., Wang J., Darzi Y., Faust K., Kurilshikov A., Bonder M. J.,
453 Valles-Colomer M., Vandeputte D., Tito R. Y., Chaffron S., Rymenans L., Verspecht C., De Sutter L.,
454 Lima-Mendez G., D’hoë K., Jonckheere K., Homola D., Garcia R., Tigchelaar E. F., Eeckhaut L., Fu
455 J., Henckaerts L., Zhermakova A., Wijmenga C., and Raes J. Population-level analysis of gut
456 microbiome variation. *Science*, 352(6285):560–4, Apr 2016. doi: 10.1126/science.aad3503.
- 457 [39] Raes J. Editorial overview: It’s the ecology, stupid: microbiome research in the post-stamp collecting
458 age. *Curr Opin Microbiol*, 44:iv–v, Aug 2018. doi: 10.1016/j.mib.2018.07.008.
- 459 [40] Stämmler F., Gläsner J., Hiergeist A., Holler E., Weber D., Oefner P. J., Gessner A., and Spang R.
460 Adjusting microbiome profiles for differences in microbial load by spike-in bacteria. *Microbiome*, 4(1):
461 28, Jun 2016.
- 462 [41] Lovell D., Pawlowsky-Glahn V., Egozcue J. J., Marguerat S., and Bähler J. Proportionality: a valid
463 alternative to correlation for relative data. *PLoS Comput Biol*, 11(3):e1004075, Mar 2015.
- 464 [42] Foster K. R. and Bell T. Competition, not cooperation, dominates interactions among culturable
465 microbial species. *Curr Biol*, 22(19):1845–50, Oct 2012. doi: 10.1016/j.cub.2012.08.005.

Box 1: Devising an estimator of bacterial load from 16S data.

Defining the estimator

To establish an estimator of bacterial load using 16S sequence data, we hypothesized that the composition of the sequencing data, in terms of host- versus bacteria-derived 16S reads, may provide information about the underlying density of bacteria. This occurs, we reasoned, because DNA templates of the two sources compete as targets during the amplification reaction, and biases towards one or the other will accrue exponentially. By this logic, the logarithm of the relative abundance of bacteria-to-host 16S counts captures information about the density of bacterial cells in the starting material. Accordingly, for each sample, we calculated the following estimator

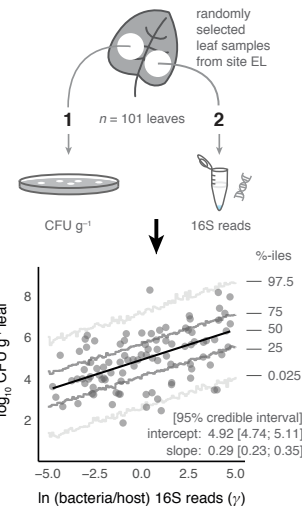
$$\gamma = \ln(r_B/r_H)$$

where r_B and r_H are the read counts of bacteria- and curated host-derived 16S counts for a given sample, respectively. r_B can be calculated at any taxonomic level, ranging from the single bASV to all of the bacteria present in the sample, by summing the sequence counts at the desired taxonomic scale.

Validating and deploying the estimator

Step 1: Collect paired tissue samples and count bacteria independently.

We validated this estimator empirically by examining the relationship between γ and an independent measure of bacterial abundance in leaf tissues derived from bacterial culturing of a subset of the samples from the EL study. These samples were surface-sterilized, homogenized, and plated on non-selective King's B media to enumerate bacterial colony forming units (CFU) per g starting leaf material, following Humphrey et al. [2014]. This approach is appropriate because a majority of bacterial taxa typically found to colonize leaf tissues can be cultivated in the laboratory on rich media [Lebeis et al., 2015; Humphrey et al., 2014].

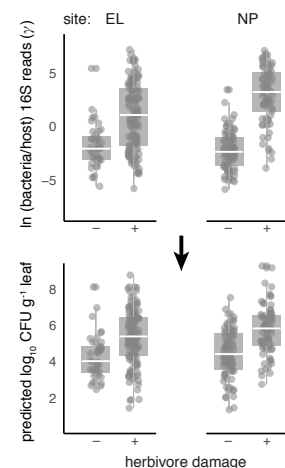


Step 2: Quantify relationship between 16S data and bacterial load.

We then estimated the slope and intercept of the relationship between observed \log_{10} CFU g^{-1} leaf tissue (hereafter log CFU) and the predictor variable γ for this sample set using a Bayesian linear regression, which allowed us to directly incorporate uncertainty in model fit into downstream analyses. We found a clear positive association between γ and log CFU, validating our usage of γ as an estimator of absolute bacterial abundance in leaf tissues.

Step 3: Model relationship between γ and herbivore damage.

We then deployed the validated estimator to test whether bacterial abundance as measured by γ was elevated in insect-damaged plant tissues. To begin, we modeled how γ varied across herbivore-damaged and undamaged leaves for various bacterial taxa. The illustrating example on the right shows that the distributions of γ calculated for all bacteria are elevated in herbivore-damaged bittercress tissues sampled from both sites EL and NP.



Step 4: Transform results for γ into predicted bacterial load.

Finally, we used posterior draws of parameters from the Step 2 model to predict how variation in γ translates into predicted bacterial load as expressed in log CFU. To the right, we can see that elevated γ in herbivore-damaged tissues translates into higher bacterial loads when predicted based on the relationship between γ and log CFU. Further details on how we specified and estimated models, as well as how we incorporated parameter uncertainty throughout this approach, can be found in *Methods: Quantifying & modeling bacterial abundance patterns*.

478 **Figures**

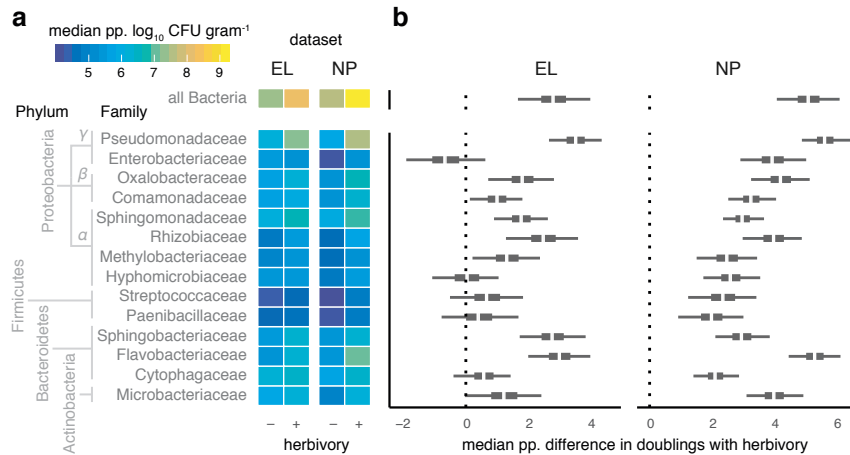


Figure 1: Pervasive increases in endophytic bacterial load in herbivore-damaged leaves. a–b. Posterior predicted (‘pp.’) infection intensity of bacterial amplicon sequence variants (bASV) from the 14 most prevalence bacterial families show variation in the extent of elevated growth in herbivore-damaged leaf tissue. **a.** Heatmap shows median predicted \log_{10} bacterial abundance (colony-forming units, CFU) per g starting leaf material) from 200 posterior simulations of the best-fitting model of each bacterial family separately (see Methods). **b.** Median (white), 95%, and 50% quantiles of the median difference in the number of predicted bacterial cell divisions (i.e., doublings) achieved in herbivore-damaged leaves compared to undamaged leaves, for sites EL and NP separately.

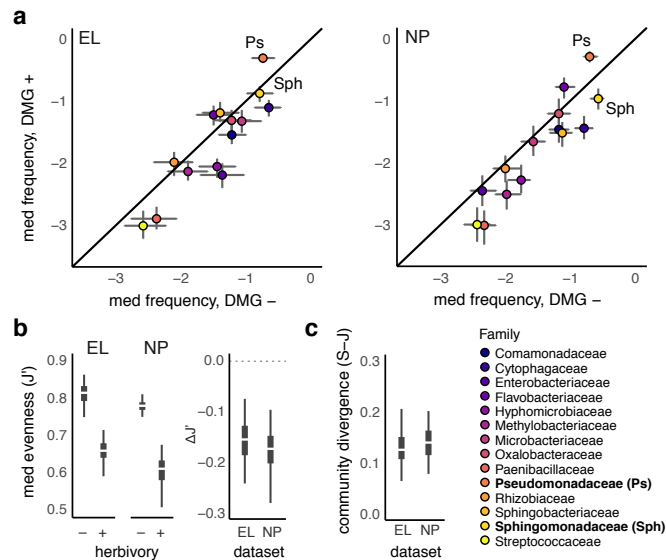


Figure 2: Herbivore-damaged leaves harbor compositionally diverged microbiomes with reduced ecological diversity shifted heavily towards Pseudomonadaceae. **a.** \log_{10} relative abundance of each family in undamaged (x -axis) versus damaged (y -axis) samples shows skew towards Pseudomonadaceae (Ps) and relative reductions of abundance among most other taxa at both study sites, including *Sphingomonas* (Sph) which shows a ~ 2 -fold increase in number of doublings in herbivore damaged leaves. **b.** Compositional changes from the amplification of already abundant taxa (e.g., Pseudomonadaceae) produces reduced community-level evenness (J') and leads to compositional divergence (i.e., β -diversity) between damaged and undamaged leaves at both study sites (**c**).

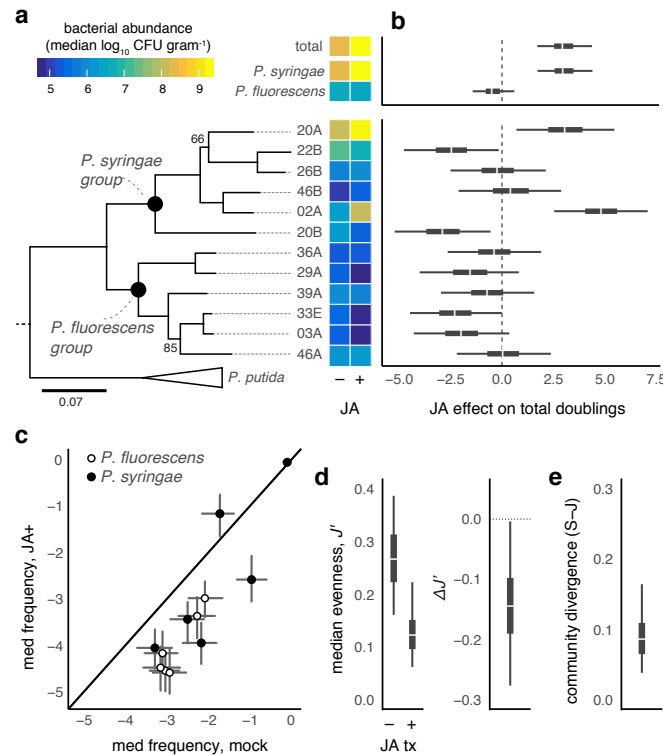


Figure 3: Eliciting plant defenses against chewing herbivores alters within-host performance of putative phytopathogens. **a.** Experimental infections with 12 *Pseudomonas* spp. strains, concurrently isolated from EL study site²⁰, show strain-to-strain variation in growth under mock-treated (M) and jasmonic acid (JA) induced plants. Heatmap shows median \log_{10} CFU g^{-1} surface sterilized plant tissue 2 d post inoculation. Maximum likelihood phylogeny of strains estimated with four housekeeping loci (2951 bp) from²⁰. **b.** Median, 95%, and 50% quantiles of the posterior difference between the number of bacterial doublings attained by bacteria growing in JA- versus mock-treated leaves (see Supplemental Methods). **c.** Compositional analysis of relative abundances calculated from (a) reflect decreased evenness (J' ; **d**) in JA-treated plant tissues, leading to overall community-level divergence (**e**). Median, 95%, and 50% quantiles from 200 posterior simulations of abundance (**c-e**) from the best-fitting model fit to data in (b).

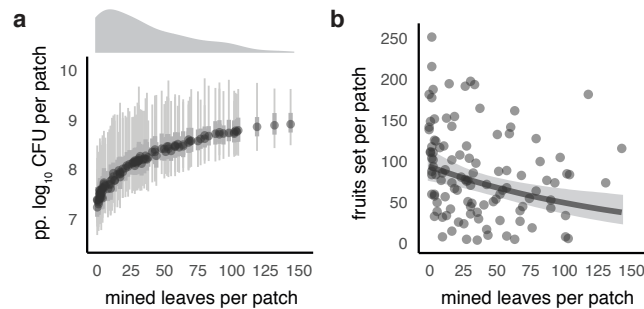


Figure 4: **Co-infection by herbivores and phytopathogenic bacteria is aggregated across plant populations and is associated with lower plant reproduction.** **a.** Median, 95%, and 50% quantiles of 200 posterior simulations of predicted ('pp.') bacterial load across plant patches ($n = 110$ at site NP; $n = 16$ stems sampled per patch). Density plot above x -axes exhibits right-skewed (i.e., aggregated) distribution of herbivore damage at the plant patch level. **b.** Patch-level herbivory (and thus co-infection intensity) is associated with decreased fruit-set in this native plant population. Plotted are raw fruit-set data summed at the patch level ($n = 16$ stems per patch), with marginal effects slope (and its 95% credible interval) plotted after accounting for average plant height (see Table S4).